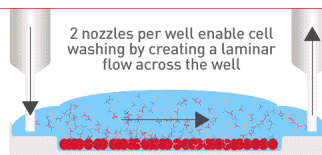


Check out how Laminar Wash systems replace centrifugation completely in handling cells



See How It Works



Immunosensitization of Tumor Cells to Dendritic Cell-Activated Immune Responses with the Proteasome Inhibitor Bortezomib (PS-341, Velcade)

This information is current as of April 22, 2019.

Lana Y. Schumacher, Dan D. Vo, Hermes J. Garban, Begoña Comin-Anduix, Sharla K. Owens, Vivian B. Dissette, John A. Glaspy, William H. McBride, Benjamin Bonavida, James S. Economou and Antoni Ribas

J Immunol 2006; 176:4757-4765; ;
doi: 10.4049/jimmunol.176.8.4757
<http://www.jimmunol.org/content/176/8/4757>

References This article **cites 47 articles**, 25 of which you can access for free at:
<http://www.jimmunol.org/content/176/8/4757.full#ref-list-1>

Why *The JI*? Submit online.

- **Rapid Reviews! 30 days*** from submission to initial decision
- **No Triage!** Every submission reviewed by practicing scientists
- **Fast Publication!** 4 weeks from acceptance to publication

**average*

Subscription Information about subscribing to *The Journal of Immunology* is online at:
<http://jimmunol.org/subscription>

Permissions Submit copyright permission requests at:
<http://www.aai.org/About/Publications/JI/copyright.html>

Email Alerts Receive free email-alerts when new articles cite this article. Sign up at:
<http://jimmunol.org/alerts>

The Journal of Immunology is published twice each month by
The American Association of Immunologists, Inc.,
1451 Rockville Pike, Suite 650, Rockville, MD 20852
Copyright © 2006 by The American Association of
Immunologists All rights reserved.
Print ISSN: 0022-1767 Online ISSN: 1550-6606.



Immunosensitization of Tumor Cells to Dendritic Cell-Activated Immune Responses with the Proteasome Inhibitor Bortezomib (PS-341, Velcade)¹

Lana Y. Schumacher,^{*||} Dan D. Vo,^{*} Hermes J. Garban,^{*} Begoña Comin-Anduix,^{*} Sharla K. Owens,^{*||} Vivian B. Dissette,^{*} John A. Glaspy,[†] William H. McBride,^{‡§} Benjamin Bonavida,^{§||} James S. Economou,^{*§||} and Antoni Ribas^{2*†§}

Proteasome inhibition results in proapoptotic changes in cancer cells, which may make them more sensitive to immune effector cells. We established a murine model to test whether the proteasome inhibitor bortezomib could sensitize established B16 melanoma tumors to dendritic cell (DC)-activated immune effector cells. Day 3-established s.c. B16 tumors had significantly decreased tumor outgrowth when treated with a combination of bortezomib and DC, regardless of whether the DC were loaded or not with a tumor Ag. In vivo Ab-depletion studies demonstrated that the effector cells were NK and CD8⁺ cells, but not CD4⁺ cells. NF- κ B nuclear transcription factor assay and gene-expression profiling of B16 treated with bortezomib was consistent with inhibition of NF- κ B target genes leading to a proapoptotic phenotype. In vitro lytic assays demonstrated that TNF- α , but not perforin, Fas-ligand, or TRAIL, was responsible for bortezomib-sensitized B16 cytotoxicity. In conclusion, the proteasome inhibitor bortezomib can pharmacologically sensitize tumor cells to the lytic effects of DC-activated immune effector cells. *The Journal of Immunology*, 2006, 176: 4757–4765.

Proteasome inhibition of cancer cells has been shown to result in a preferential proapoptotic phenotype. The proapoptotic activity of bortezomib (Velcade, formally known as PS-341) results in clinical responses in patients with chemotherapy-resistant multiple myeloma (1). This led to its licensing by the Food and Drug Administration in 2003. Bortezomib is a boronic acid dipeptide derivative which forms a covalent and reversible bond with the proteasome, selectively inhibiting the chymotrypsin-like activity of the proteasome (2). Malignant cells are more susceptible to treatment with proteasome inhibitors possibly because of their stronger dependency on proteasome-regulated stress-related pathways such as proliferation, cell cycle, and apoptosis (2). Work by Murphy and colleagues (3) at the University of Nevada (Reno, NV) has demonstrated that bortezomib could sensitize target cells to death receptor-mediated apoptosis, leading to enhanced immune-mediated graft-vs-tumor effects without worsening graft-vs-host-disease (4). For these reasons, we hy-

pothesized that bortezomib could be a candidate drug to pharmacologically enhance cancer cell sensitivity to immunotherapy.

The principal cytolytic immune effector cells are T cells and NK cells, both of which recognize their targets using specific receptors through partially complementary mechanisms. T cells recognize Ag presented by surface self-MHC molecules through their TCR (5), while NK cells recognize their targets through the absence of syngeneic MHC molecules through the dominant NK-inhibiting receptors, or the presence of allogeneic MHC molecules or MHC-like molecules by NK-activating receptors (6, 7). In general, target cells that express a cognate Ag/MHC complex for an activated T cell will be susceptible to CTL, while if the cells down-regulate MHC expression (as frequently occurs during viral infections or in malignancy), they then become less susceptible to lytic activity by CTL but will become more susceptible to NK cells. However, there is promiscuous expression of innate activating receptors among lytic cells, and the boundary between T and NK cells seems vague (8, 9). Immune effector cells induce apoptotic death of their susceptible targets through two common pathways: the perforin/granzyme B pathway and the TNFR superfamily of death receptors (TNF- α , Fas, TRAIL). Upon immune effector cell target recognition through the TCR or NK-activating receptors, cytotoxic granules containing perforin and granzyme B are released, resulting in membrane pore formation and granzyme B activation of the intrinsic and extrinsic apoptotic cascade resulting in cytotoxic death of target cells within a short period of time (<4 h) (10, 11). The same signals may result in the more protracted release of the soluble factor TNF- α , or the surface expression of FasL and TRAIL, which require the expression of their specific receptors on the target cells. Engagement of TNFR, FasR, or TRAIL receptors D4 and D5 on the target cell surface, together with the recruitment of adaptor molecules, results in the activation of the extrinsic pathway of apoptosis and delayed cytotoxic death of target cells (over 12 h) (10–12).

^{*}Department of Surgery, Division of Surgical Oncology, [†]Department of Medicine, Division of Hematology-Oncology, [‡]Department of Experimental Radiation Oncology, [§]Jonsson Comprehensive Cancer Center, and ^{||}Departments of Microbiology, Immunology, and Molecular Genetics, University of California, Los Angeles, CA 90095; and ^{||}Department of Surgery, Stanford University Hospital, Stanford, CA 94305

Received for publication March 23, 2005. Accepted for publication January 27, 2006.

The costs of publication of this article were defrayed in part by the payment of page charges. This article must therefore be hereby marked *advertisement* in accordance with 18 U.S.C. Section 1734 solely to indicate this fact.

¹ This work was supported in part by National Institutes of Health (NIH)/National Cancer Institute Grants RO1 CA77623, RO1 CA79976, T32 CA75956, and K12 CA76905, the Stacy and Evelyn Kesselman Research Fund, and the Monkarsh Fund (to J.S.E.); and Stop Cancer Career Development Award, K23 CA93376, P50 CA086306, and a University of California Los Angeles (UCLA) Human Gene Medicine Seed Grant Award (to A.R.). Flow cytometry was performed in the UCLA Jonsson Comprehensive Cancer Center and Center for AIDS Research Flow Cytometry Core Facility that is supported by NIH Awards CA-16042 and AI-28697.

² Address correspondence and reprint requests to Dr. Antoni Ribas, Division of Hematology-Oncology, UCLA Medical Center, 11-934 Factor Building, 10833 Le Conte Avenue, Los Angeles, CA 90095-1782. E-mail address: aribas@mednet.ucla.edu

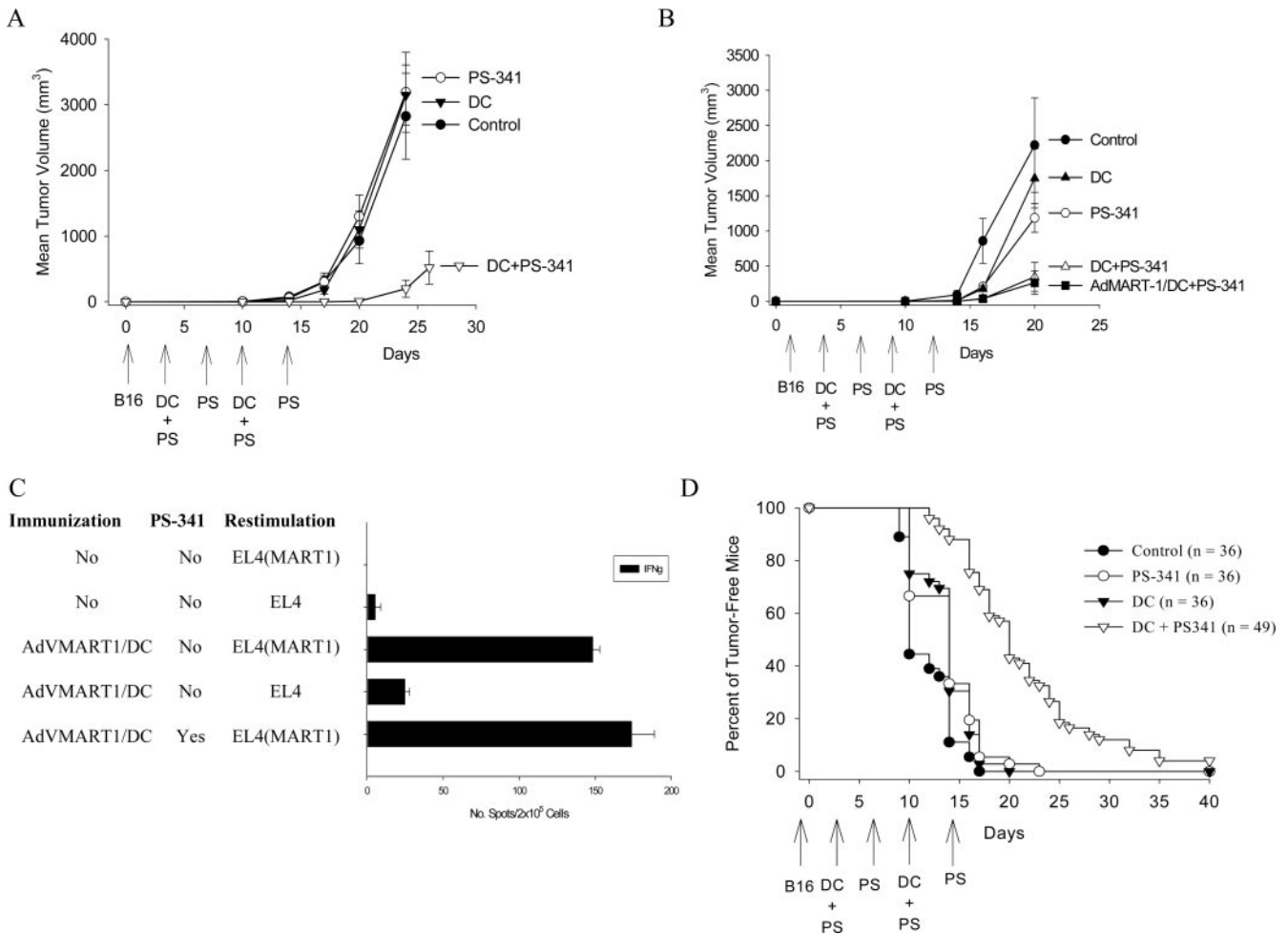


FIGURE 1. Treatment of established B16 with combined DC vaccines and bortezomib. *A*, Treatment of established murine tumors with combined AdVMART1-transduced DC (AdVMART1/DC) and bortezomib. B16 tumors were implanted in the flanks of mice. Starting 3 days later, groups of five mice were treated with AdVMART1/DC s.c. (days 3 and 10) and bortezomib i.p. (days 3, 7, 10, and 13). The graph represents tumor volume over time after B16 implantation. *B*, Ag nonspecificity. Mice had B16 tumors implanted and were allocated into groups of five mice. Each group received either AdVMART1/DC or untransduced DC, in both cases in conjunction with bortezomib following the same schedule as in *A*. *C*, Lack of adverse effects of bortezomib on MART-1-specific T cells. Splenocytes from mice treated with or without AdVMART1/DC combined with bortezomib, as indicated, were harvested on day 14 after study initiation. RBC-depleted splenocytes were restimulated *in vitro* with EL4 cells stably transfected with MART-1 (EL4-MART1) or parental cells not expressing MART-1 (EL4) for 48 h, after which cells were added to an IFN- γ ELISPOT plate. *D*, Treatment of established murine tumors with combined DC and bortezomib. Kaplan Meier plot of percent tumor-free mice over time combining data from eight independent replicate studies ($p < 0.0001$).

We hypothesized that the pharmacological inhibition of tumor proteasome enzymatic activity would sensitize tumor cells to immune effectors. To test this hypothesis, we developed an *in vivo* murine model treating established B16 melanoma with a combined therapy of dendritic cell (DC)-based immunization/activation and the proteasome inhibitor bortezomib. Tumor growth was significantly delayed in mice treated with the combined therapy as opposed to either therapy alone. DC-based tumor suppression was Ag independent and required both NK and CD8⁺ T cells but not CD4⁺ T cells. *In vitro* correlative studies suggested that lytic activity was mediated by TNF- α .

Materials and Methods

Mice

C57BL/6, and CD8 α -chain knockout mice (CD8KO) in a C57BL/6 background (B6.129S2-Cd8 α^{tm1Mak} , backcrossed >28 generations), were purchased from The Jackson Laboratory and were bred and kept under de-

finied-flora pathogen-free conditions at the Association for Assessment of Laboratory Animal Care-approved Animal Facility of the Division of Experimental Radiation Oncology (University of California, Los Angeles, CA; UCLA). Mice were handled in accordance with the UCLA animal care policy.

Cell lines and MHC surface staining

B16-F0 (B16), a murine melanoma, EL4, a murine lymphoma, and Yac-1, a murine lymphoma, were obtained from the American Type Culture Collection (ATCC). B16 and EL4 were maintained *in vitro* in DMEM (Invitrogen Life Technologies), and Yac-1 in RPMI 1640 (Invitrogen Life Technologies), in both cases supplemented with 10% FCS (Gemini) and 1% (v/v) penicillin, streptomycin, and amphotericin (Gemini). Generation of EL4 (MART1) stable transfectants has been previously described (13). Stably transfected cells were maintained *in vitro* under constant G418 selection (0.5 mg/ml; Invitrogen Life Technologies). Determination of surface expression of MHC class I molecules was performed by cell surface staining with a PE-conjugated anti-H2-K^b Ab (BD Pharmingen). Staining was analyzed by flow cytometry.

Reagents

Bortezomib (Velcade), a dipeptide boronic acid proteasome inhibitor, was purchased or was a gift (in some experiments) from Millennium Pharmaceuticals. Bortezomib was prepared as a stock solution in 0.9% saline. For

³ Abbreviations used in this paper: DC, dendritic cell; LAK, lymphocyte-activated killer; LDH, lactate dehydrogenase; AMC, 7-amido-4-methylcoumarin.

administration to animals, stock solutions were thawed and further diluted in 0.9% saline to a dilution to yield 0.02 mg/0.1 ml (1 mg/kg/mouse) for i.p. injection. Purified hamster anti-mouse Fas mAb (Jo2) and recombinant mouse TNF- α were purchased from BD Pharmingen. Stock solutions of reagents were routinely prepared in PBS or medium as appropriate.

Proteasome function assay

Proteasome function was measured as described previously (14) with some minor modifications. Briefly, B16 melanoma cells were treated with or without 150 nM bortezomib for 3 h. The cells were then washed with 1 \times PBS (pH 7.2), then with buffer I (50 mM Tris (pH 7.4), 2 mM DTT, 5 mM MgCl₂, 2 mM ATP), and pelleted by centrifugation. Homogenization buffer (50 mM Tris (pH 7.4), 1 mM DTT, 5 mM MgCl₂, 2 mM ATP, 250 mM sucrose) was then added and cells underwent three freeze-thaw vortex cycles with liquid nitrogen and a 37°C water bath. Cell debris was next removed by centrifugation at 4°C, 1,000 \times g for 5 min and 10,000 \times g for 25 min and supernatant was transferred to new Eppendorf tubes. Twenty micrograms of protein of each sample was diluted with buffer I to a final volume of 200 μ l. The fluorogenic proteasome substrates SucLLVY-MCA (chymotrypsin-like; Sigma-Aldrich), Z-Leu-Leu-Leu-AMC (Calbiochem), and Boc-Val-Leu-Lys-AMC (trypsin-like; Sigma-Aldrich) were dissolved in DMSO and added in a final concentration of 80 μ M (0.8% DMSO). Proteolytic activity was monitored continuously by the release of the fluorescent group 7-amido-4-methylcoumarin (AMC) measured in a fluorescence plate reader (Spectrafluor (Tecan) and Spectra Max Gemini XS (Molecular Devices), 37°C) at 380/460 nm. In control experiments using MG-132, the chymotryptic activity of the lysates was always inhibited by >90%, indicating that the observed cleavage activity was mainly based on proteasome function.

Cell viability assay

Cell viability upon treatment with bortezomib was determined by the MTT assay, as described (15). A total of 25 \times 10³ B16 cells/well was incubated in 96-well plates in the presence or in the absence of bortezomib at the specified concentrations. The blue MTT formazan precipitate was dissolved in 100 μ l of Me₂SO, and the absorbance values at 565 nm were determined on a multiwell plate reader. Murine melanoma B16 cell cultures used in this study were free of mycoplasma, tested using a *Mycoplasma* PCR ELISA kit (Roche Diagnostic).

Recombinant adenoviruses

The replication-deficient adenoviral vector AdVMART1 is a previously described E1-deleted vector based on human type 5 adenovirus (16). It contains the 400-bp human MART-1 cDNA driven by the CMV early enhancer/promoter.

Preparation of DC and adenoviral transduction

DC were differentiated from bone marrow progenitor cells derived from C57BL/6 mice by *in vitro* culture in murine GM-CSF (100 ng/ml; Amgen) and murine IL-4 (500 U/ml; R&D Systems) as described by Inaba et al. (17) with minor modifications (16). DC were harvested as loosely adherent cells, washed twice in PBS (Mediatec), and immediately prepared for injection in 0.2 ml of PBS/mouse. When indicated, DC were transduced in RPMI 1640 with 2% FCS transduction media at a multiplicity of infection of 100 viral PFU/each DC. Transduction was conducted for 2 h at 37°C, after which time 5 vol of 10% FCS RPMI 1640 medium was added to neutralize free virus, and then the adenovirally transduced DC were washed twice in PBS and resuspended in 0.2 ml of PBS/animal for injection (16, 18).

Animal studies

B16 cells used for tumor challenge were obtained from single-cell suspensions of progressively growing tumors in syngeneic mice to avoid the confounding effects of the presentation of medium- and serum-deprived epitopes. To generate single-cell suspensions, tumors were surgically removed, decapsulated, and minced. Minced tumors underwent enzymatic digestion for 2 h with DNase (0.1 mg/ml; Sigma-Aldrich) and collagenase D (1 mg/ml; Roche Applied Sciences) in 50 ml of AIM-V medium (Invitrogen Life Technologies). Viable cells were washed three times in PBS and resuspended in 0.1 ml of PBS/animal (16, 18). Tumors were injected s.c. into the left flank (1 \times 10⁵ cells/injection) on day 0. Injected cells were >70% viable, as determined by trypan blue exclusion. On days 3 and 10, mice received untransduced DC or DC transduced with AdVMART-1 (0.5–1.0 \times 10⁶ cells/injection) s.c. in the right flank. Bortezomib was administered at 1 mg/kg/mouse i.p. on days 7, 10, and 14. Each treatment group typically contained five mice.

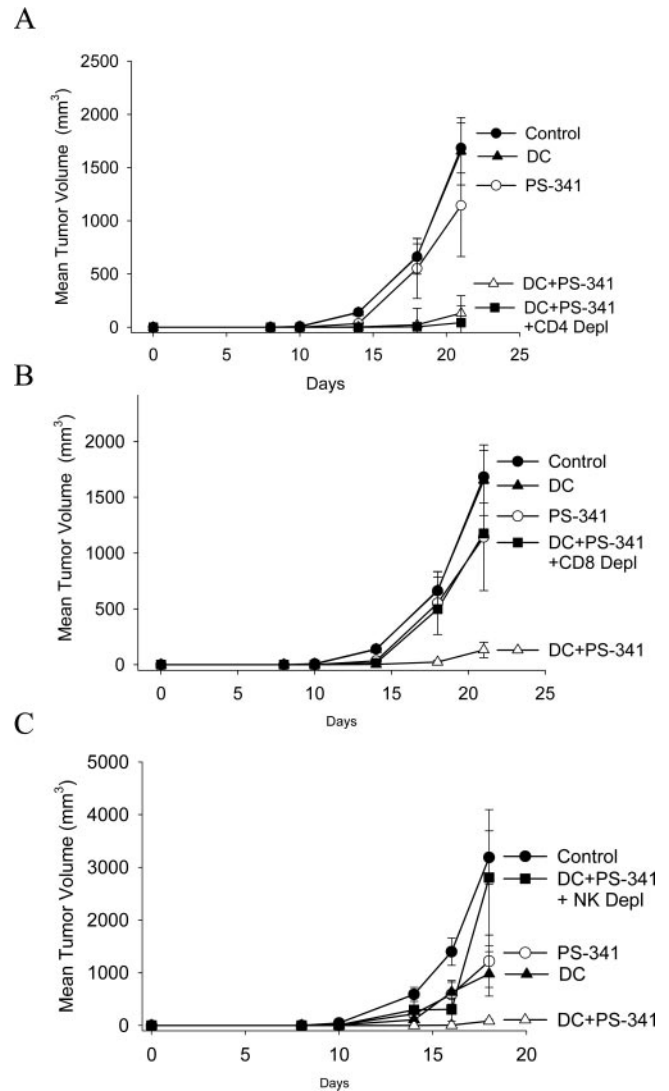


FIGURE 2. CD8 and NK cells mediate the antitumor effects of DC plus bortezomib. Groups of five mice were depleted of CD4 cells (A), CD8 cells (B), or NK cells (C) using specific Abs as described in *Materials and Methods*. B16 tumors were then implanted s.c. in a flank and mice received combined DC plus bortezomib therapy. In all studies, tumor outgrowth after administration of DC or bortezomib alone was not different from control mice at the $p = 0.05$ significance level, while DC plus bortezomib was significantly different in all studies. Depletion of CD4 cells did not abrogate the antitumor effects of the combination, while depletion of CD8 and NK cells did abrogate the antitumor activity.

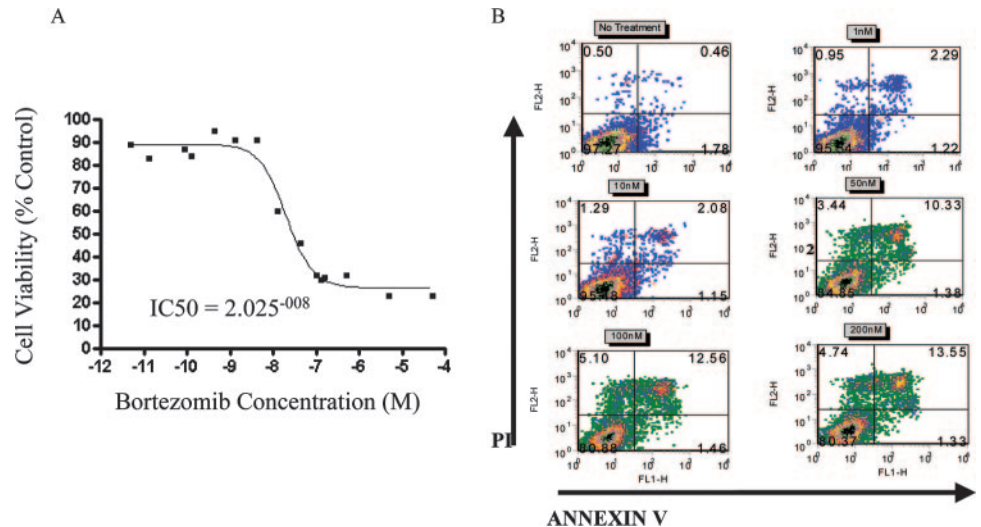
Immune cell subset depletion *in vivo*

In vivo Ab ablation of CD8⁺ (clone 2.3), CD4⁺ (clone GK1.5) T cell subsets, and NK1.1⁺ (clone PK136) cells was performed by i.p. injection of 100–200 μ g of purified endotoxin-free Ab/mouse/injection (BioExpress) on days -5, -3, and -1 before tumor inoculation, and every 6 days thereafter. Monitoring of successful depletion was performed by flow cytometry on splenocytes harvested on the day of tumor inoculation for CD4⁻ and CD8-depleting Abs. NK depletion was confirmed by NK cell activity microcytotoxicity assays using the NK-sensitive Yac-1 cell line as target cells and IL-2-activated lymphocyte-activated killer (LAK) cells as effectors (Yac-1 assay) (19).

DC phenotyping

Bone marrow-derived DC were evaluated after an 8-day culture in GM-CSF and IL-4 and were treated for 18 h with a dose titration of bortezomib at 200, 100, 10, and 1 nM. DC were then stained with H2-K^b PE anti-mouse (MHC class I molecule), CD86 PE anti-mouse, CD80 FITC

FIGURE 3. Proapoptotic effects of bortezomib on B16 melanoma in vitro. *A*, B16 cultures were treated in vitro with increasing concentrations of bortezomib. Their viability was determined by formazan dye uptake and expressed as percentage of untreated control cell viability (results are the mean of nine experiments). *B*, B16 melanoma cells were treated in vitro with a dose titration of bortezomib for 18 h. Apoptotic and necrotic cell death was assessed by double staining using annexin V and PI, and read using flow cytometry.



anti-mouse, CD11c PE anti-mouse (all from BD Pharmingen), and I-A^b FITC anti-mouse (MHC class II molecule; Caltag Laboratories). Stained cells were analyzed by flow cytometry. DC were also stained with annexin V (BD Pharmingen) according to the manufacturer's instructions.

Cytokine profile by ELISPOT

For the detection of MART-1 Ag-specific responses, splenocytes depleted of RBC by hypotonic lysis, cultured in vitro with irradiated EL4 or EL4 (MART-1) at a 25:1 ratio for 48 h in the presence of 10 U/ml IL-2, were added in duplicate 3-fold dilutions to 96-well mixed cellulose plates (Multiscreen filtration system; Millipore) precoated with anti-IFN- γ Ab (BD Pharmingen). For Ag-nonspecific responses, RBC-depleted splenocytes were added directly to IFN- γ -coated plates with or without the addition of PMA (Sigma-Aldrich). Plates were incubated for 24 h at 37°C. Spots were developed using a secondary biotin-labeled Ab and counted under a dissecting microscope as previously described (20).

⁵¹Cr in vitro cytotoxicity assay

For short-term in vitro microcytotoxicity assays, RBC-depleted splenocytes, harvested 3 days after bortezomib treatment, were cultured in vitro for 96 h at the same conditions described above for ELISPOT assays, and assayed in a standard 4-h chromium release test as we have previously described (21).

Lactate dehydrogenase (LDH) in vitro cytotoxicity assay

The LDH-based CytoTox 96 Assay (Promega) was used to determine in vitro cytotoxicity as described previously. Briefly, 5×10^3 to 7×10^3 cells/sample, in quadruplicate, were cultured into a 96-well flat-bottom microtiter plate (Costar) and cultured at low serum concentration (0.1% FBS) 18 h before each treatment. The medium was then changed to complete DMEM with 5% heat-inactivated FBS. B16 or EL4 cells were then cultured in the presence of bortezomib at the specified concentrations. After 18 h of incubation with bortezomib, increasing concentrations of the Fas agonistic Ab Jo2, TRAIL ligand, or mouse recombinant TNF- α were added (Axxora). The assay plates were incubated for 24 h at 37°C in 5% CO₂. After incubation for each different experimental condition, released LDH into the culture supernatants was measured with a 30-min coupled enzymatic assay, which results in the conversion of a tetrazolium salt (INT) into a red formazan product that is read at 490 nm in an automated plate reader (Emax; Molecular Devices). Percentage cytotoxicity was calculated using the spontaneous release-corrected OD as follows: percent cytotoxicity = (OD of experimental well/OD of maximum release control well) \times 100.

NF- κ B-related subunits DNA-binding assay

The nuclear DNA-binding activity of the NF- κ B-related subunits p50, p52, p65 (RelA), c-Rel, and RelB was assessed using a nonisotopic quantitative assay (BD TransFactor NF- κ B family kit; BD Clontech). A total of 20 μ g of nuclear extract (prepared as we have reported previously, Ref. 22) from B16 mouse melanoma cells, treated in the absence or presence of the proteasome inhibitor bortezomib at 10 nM, were bound to microwells coated with NF- κ B consensus oligonucleotide. Wells were incubated with specific

Abs against p50, p52, p65 (RelA), c-Rel, or RelB, followed by the secondary HRP-conjugated and tetramethylbenzidine-based colorimetric-allowed detection system. Binding was quantified by the background-corrected visible absorbance at 650 nm (22).

Apoptosis microarray profiling

Total RNA was extracted and purified from $\sim 1 \times 10^6$ B16 cells cultured in the absence or presence of bortezomib (10 nM) for 18 h by a single-step monophasic solution of phenol and guanidine isothiocyanate-chloroform using TRIzol reagent (Invitrogen Life Technologies). Three micrograms of total RNA were reverse transcribed into biotin-16-deoxy-UTP-labeled single-strand cDNA using the TrueLabeling-RT kit (SuperArray Bioscience). A mouse apoptosis-focused expression microarray (SuperArray Bioscience) was individually hybridized with the biotin-labeled single-strand cDNA probe from each experimental condition in a rotating hybridization incubator overnight at 60°C and further incubated with alkaline-phosphatase-conjugated streptavidin, as per manufacturer's recommendations. Chemiluminescence signals were visualized by autoradiogram and their relative intensity was assessed by densitometric analysis of the digitized image (ScanAlyze Microarray Image Analysis, <http://rana.lbl.gov/Eisen-Software.htm>) after housekeeping gene-based normalization, background subtraction, and statistical significances determination (GEArray software; SuperArray Bioscience).

Results

Bortezomib treatment permits tumor suppression of established B16 melanoma by DC-based immunotherapy

C57BL/6 mice immunized with DC engineered to express MART-1 melanoma Ag are partially protected from a challenge of B16 melanoma, which express MART-1. This model has been extensively studied by our group (13, 19–21, 23, 24). MART-1-engineered DC can partially or completely protect mice from a subsequent B16 challenge, but we have never been successful in having any impact on even microscopically established tumors (13).

We set up a treatment model to determine whether systemic bortezomib treatment of microscopically established B16 would render them more sensitive to DC-based immunotherapy. Mice received 10^5 B16 implanted s.c. in one flank. On days 3 and 10, they received 10^6 immature DC (7-day cultures of GM-CSF/IL-4-differentiated bone marrow progenitors) transduced with an adenoviral vector expressing MART-1 (AdVMART1, multiplicity of infection 1:100) administered s.c. in the contralateral flank. Mice also received bortezomib at 1 mg/kg i.p. on days 3, 7, 10, and 14. Neither AdVMART1/DC nor bortezomib alone had any impact on B16 tumor development or growth kinetics (Fig. 1A). However,

their combination significantly delayed tumor appearance and retarded tumor growth kinetics. Three replicate studies were performed with similar results.

Bortezomib-facilitated DC tumor suppression is Ag nonspecific

We and others have shown that DC-based immunotherapy can induce both adaptive and innate antitumor responses (19, 24–29). Administration of unmodified GM-CSF/IL-4 DC to B16-bearing, bortezomib-treated mice provided a comparable degree of tumor suppression as was observed with MART-1-transduced DC (Fig. 1B). We confirmed by IFN- γ ELISPOT analysis that the administration of AdVMART1/DC expanded MART-1-specific T cells in these mice (Fig. 1C), but these tumor Ag-specific effectors were not required for the antitumor effect of DC-bortezomib combined therapy. Pooled data from eight replicate studies using a total of 157 mice demonstrated that tumor appearance was consistently delayed by \sim 10 days, but essentially all mice developed tumors (Fig. 1D).

NK and CD8⁺ T cells, but not CD4⁺ T cells, are required

CD8, CD4, or NK cells were depleted by Ab before tumor implantation and DC-bortezomib treatment. As shown in Fig. 2, CD4 depletion had no impact on tumor protection, while depletion of CD8 or NK1.1-positive cells completely abrogated tumor suppression. In summary, bortezomib treatment of B16-bearing mice facilitates tumor suppression by CD8 and NK cells driven by immature DC.

B16 melanoma treated with bortezomib acquires a proapoptotic phenotype and is sensitized to TNF- α but not perforin or FasL killing

Our hypothesis is that bortezomib sensitizes B16 to immune effectors. We sought to confirm the work of others that tumor cells acquired a proapoptotic phenotype with proteasome inhibition. In preliminary studies, we determined that the IC₅₀ of B16 treated for 24 h with bortezomib was 20 nM in an in vitro MTT assay (Fig. 3A). Also, a range of concentrations of bortezomib (1, 10, 50, 100, 200 nM) was tested to define its ability to induce apoptotic death in B16 cells in vitro. There was a concentration- and time-dependent increase in annexin V and propidium iodine single- and double-positive cells, demonstrating apoptotic death of B16 with increasing bortezomib exposure (Fig. 3B).

Using a sublethal concentration of 10 nM of bortezomib, we sought to determine the effects of proteasome inhibition on the differential gene expression pattern from bortezomib-untreated (Fig. 4A) and -treated (Fig. 4B) mouse melanoma B16 cells, using a mouse pathway-focused gene expression microarray corresponding to 96 key apoptosis-related genes. The following transcripts were up-regulated with bortezomib (Fig. 4B, solid boxes): Bcl2/adenovirus E1B 19kDa-interacting protein 1, NIP3 (*Bnip3*), a proapoptotic member of the Bcl-2 family (30, 31); transformed mouse 3T3 cell double minute 2 (*Mdm2*), a p53-related apoptosis regulator with both pro- and antiapoptotic activities (32); and nucleolar protein 3 (*Nol3*), an apoptosis repressor with a caspase recruitment domain domain (33). Four genes were found to be significantly down-regulated by bortezomib (Fig. 4B, dotted boxes): baculoviral inhibitor of apoptosis protein (IAP) repeat-containing 5 (*Birc5*, *Survivin*), a critical antiapoptosis regulator (34); replication protein A3 (*Rpa3*), a DNA stability/cell cycle checkpoint regulator (35); TNFR-associated factor 4 (*Traf4*), a NF- κ B-associated antiapoptosis gene (36); and transformation-related protein 53 (*Trp53*), a cell cycle-related anti-apoptosis gene (37).

Immune effector cells, including T, NK, and LAK cells, kill targets either through the release of perforin/granzyme B resulting

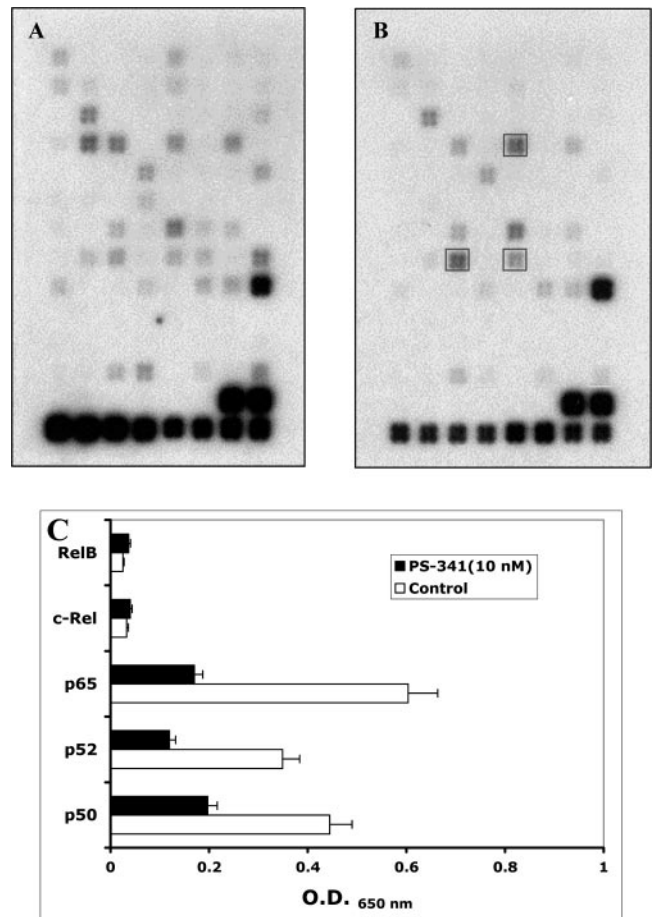


FIGURE 4. Bortezomib-induced differential apoptosis-related gene expression in B16 cells and inhibition of NF- κ B-related DNA binding activity. B16 cells were cultured in the absence (A) or presence (B) of PS-341 (10 nM) for 18 h. Total RNA was isolated, reverse-transcribed into biotin-16-dUTP-labeled single-strand cDNA, and hybridized to pathway-focused gene expression (apoptosis-related) microarray membranes. Chemiluminescence signal was visualized by autoradiography, digitized, and analyzed after normalization of gene expression using *Gapd* and *Actb* genes. Significant up-regulated transcripts in solid boxes (from top to bottom/left to right: *Bnip3*, *Mdm2*, and *Nol3*), and down-regulated transcripts in dotted boxes (from top to bottom/left to right: *Birc5*, *Rpa3*, *Traf4*, and *Trp53*). C, Nuclear extracts from B16 mouse melanoma cells, treated in the absence or presence of bortezomib (10 nM), were analyzed for specific DNA-binding activity of the NF- κ B-related subunits p50, p52, p65 (RelA), c-Rel and RelB. Results are expressed as their background-corrected absorbance at 650 nm \pm SEM ($n = 4$) using a colorimetric-based protein DNA-binding assay.

in target cell death in short-term (4 h) in vitro assays, or the engagement of the TNFR family of death receptors that require longer assays to detect cytotoxicity. Both pathways activate the extrinsic and intrinsic apoptotic machinery, eventually resulting in the activation of effector caspases and target cell apoptotic death. We tested whether bortezomib would sensitize target cells to perforin-mediated killing in 4-h chromium release assays. We tested the lytic activity of DC and IL-2-stimulated lytic cells against B16, with or without bortezomib treatment, compared with the lytic activity against Yac-1 as a positive control. Splenocytes from DC-administered mice, regardless of exposure to high concentrations of IL-2 in vitro to generate LAK cells with NK lytic activity, had low lytic activity to B16 in a short-term microcytotoxicity assay. Only splenocytes cultured in IL-2 ex vivo had lytic activity to the

NK-preferred target Yac-1, while splenocytes from DC-administered mice did not demonstrate NK lytic activity under these assay conditions (Fig. 5A). To further confirm the lack of sensitization to perforin-mediated killing, we turned to a CD8^{null} environment with enhanced NK responses to DC administration. We have previously reported that administration of DC to CD8KO mice results in the activation of much higher levels of NK effector cell lytic activity than when administered to wild-type mice. These NK effectors lyse B16 through the perforin pathway (19). Therefore, we administered DC to CD8KO mice and tested their ability to lyse chromated B16 targets with or without prior bortezomib treatment. Again, killing of B16 treated with bortezomib, if anything, was decreased compared with untreated B16 targets and Yac-1 (data not shown). In conclusion, no target cell sensitization by bortezomib to NK lytic activity could be detected in short-term microcytotoxicity assays, which predominantly detect perforin-mediated target cell killing.

We then tested the *in vitro* sensitivity to the three death receptor ligands in long-term LDH release microcytotoxicity assays. The death receptor pathway requires longer exposure than when assessing perforin-mediated killing in standard 4-h chromium release assays. We used EL4 lymphoma as a positive control for Fas, TRAIL, and TNF- α -mediated killing in this assay. Sublytic doses of FasR-activating Ab or TRAIL ligand, with or without concurrent bortezomib at 10 nM, a concentration below the IC₅₀ for B16,

did not result in significant killing of B16 (Fig. 5, C and D). On the contrary, the combination of TNF- α and bortezomib resulted in increased killing of B16 (Fig. 5B), a cell line that has been previously shown to be resistant to TNF- α -mediated killing (38). In conclusion, these functional assays suggest that bortezomib sensitizes B16 cells to killing through TNF- α receptor engagement. These findings confirm those of Murphy and colleagues (3, 4) and collectively provide circumstantial support for our immunosensitization hypothesis.

Bortezomib has no significant impact on several immune effector functions

An alternative hypothesis is that bortezomib enhances immune effector cell function to produce this antitumor response. We could find no evidence to support this. As already shown in Fig. 1C, the expansion and activation of Ag-specific T cell responses are unaffected by the dose and treatment schedule of the proteasome inhibitor we used. *In vitro* treatment of DC with bortezomib did decrease MHC class I expression, less markedly for MHC class II, and had no effect on expression of costimulatory molecules CD80 and CD86 or the adhesion molecule CD11c (Fig. 6A). There was evidence of early apoptosis in DC starting at 10 nM concentrations of bortezomib using the marker annexin V (Fig. 6B). Finally, spleen cells from bortezomib-treated mice were not enhanced nor impaired in their ability to be stimulated by PMA to produce

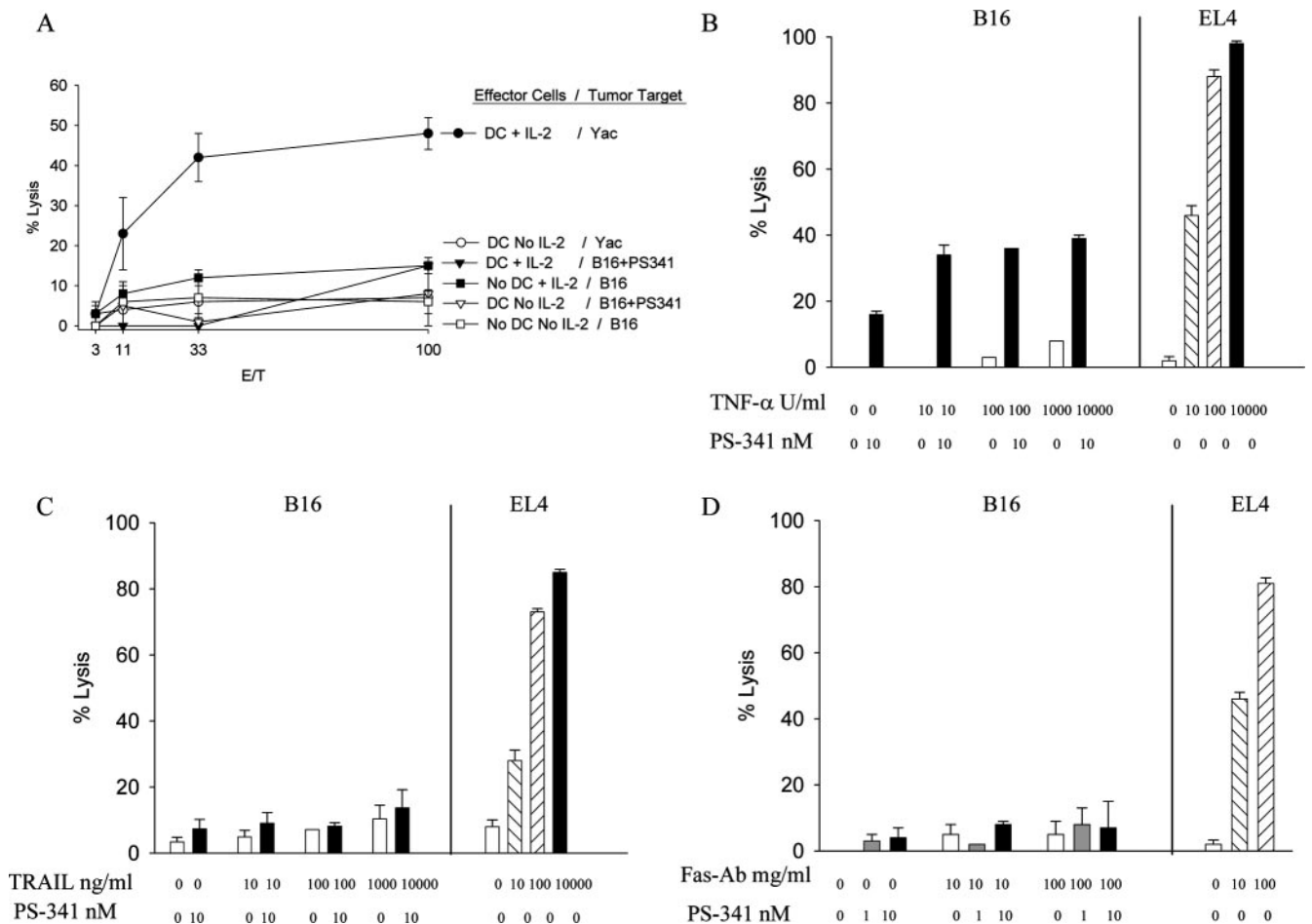


FIGURE 5. Mechanism of target cell killing by DC-activated effector cells on bortezomib-treated B16 targets. *A*, Four-hour ⁵¹Cr release assay using DC-activated splenocytes from C57BL/6 mice cultured overnight in 10⁴ IU of IL-2 (LAK cells) or without IL-2 (no IL-2 group), and assayed for lytic activity to Yac-1 cells or B16 cells. *B–D*, Long-term (18 h) LDH release assay using B16 cells and EL4 lymphoma cells (as a positive control for death receptor ligand-mediated cytotoxicity) cultured in different concentrations of bortezomib and different concentrations of soluble TNF- α (*B*), TRAIL ligand (*C*), and the anti-Fas Ab Jo2 (*D*).

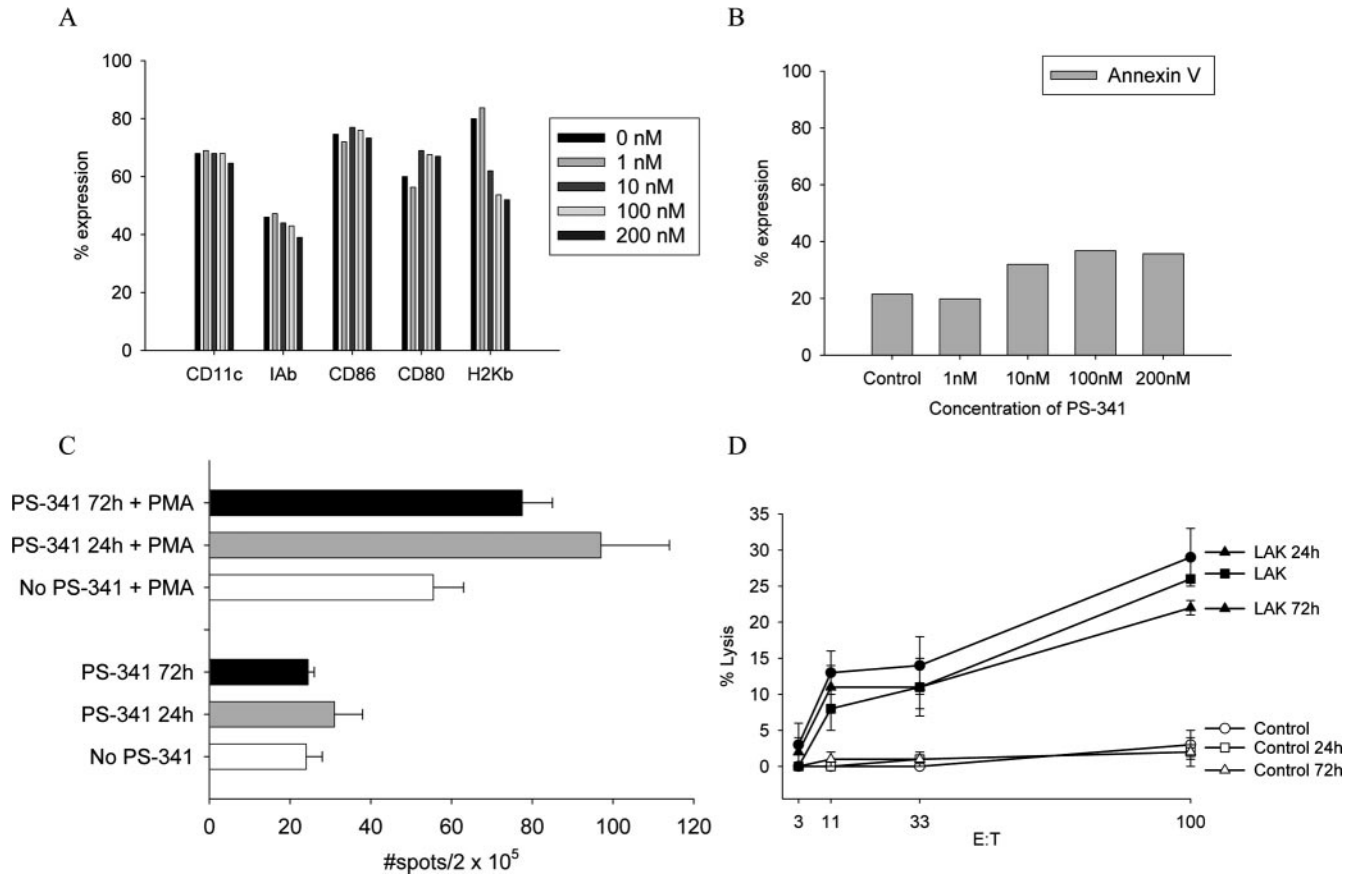


FIGURE 6. Effects of bortezomib on DC immune effector cell function. GM-CSF and IL-4-differentiated immature DC were cultured with different concentrations of bortezomib for 18 h. Cells were harvested and surface stained with fluorochrome-labeled Abs (A) or were stained for apoptotic cells by annexin V (B). Results were concordant in three replicate studies. C, RBC-depleted splenocytes from naive mice or mice treated i.p. with bortezomib (1 mg/kg) 24 or 72 h earlier were harvested and cultured in the presence or absence of PMA. Non-Ag-specific IFN- γ production was determined by ELISPOT. D, Splenocytes from the same mice were cultured overnight in 10^4 IU of IL-2, which generates LAK cells, and their lytic activity to target Yac-1 cells was determined in a 4-h chromium release assay.

IFN- γ or to generate IL-2-activated lytic NK cells (Fig. 6, C and D). In summary, there appeared to be a modest impact of the proteasome inhibitor on cells from the innate and adaptive responses in the models we studied.

Discussion

Tumor cells acquire a variety of mechanisms for resistance to apoptosis induced by immune effector cells (39, 40). The improved understanding of these pathways, together with the development of specific inhibitors for critical molecules responsible for tumor resistance, may facilitate the reversal of tumor escape from the immune system (40, 41). The ubiquitin-proteasome pathway plays an important role in regulating the degradation of proteins involved in the cell cycle, cell survival, transcriptional activation, and tumor growth. Many proteasome substrates are known mediators of pathways that are dysregulated in neoplasia. Proteasome substrates include signaling molecules, tumor suppressors, cell-cycle regulators, transcription factors, inhibitory molecules (degrading these molecules in turn activate other molecules), and antiapoptotic proteins (42). Altering the function of the proteasome and disrupting the degradation of these proteins have profound effects on cell growth and survival, particularly in rapidly dividing cancer cells, which require increased availability of growth-promoting proteins (43). Inhibiting the proteasome modulates the function of critical cellular molecules, such as the tumor suppressor p53 and the cyclin-dependent kinase inhibitors p21 and p27 (2). Its best-charac-

terized effect is in the modulation of the transcriptional factor NF- κ B. The activity of NF- κ B is regulated by proteasome-mediated degradation of the inhibitor protein I κ B. In response to stress such as neoplasia, I κ B becomes phosphorylated and deactivated by the proteasome thus promoting NF- κ B-induced prosurvival pathways. Therefore, when the proteasome is inhibited, I κ B in turn inhibits the activation of NF- κ B thus affecting the role of NF- κ B in anti-apoptosis, tumor metastasis, and angiogenesis (44). The inhibition of NF- κ B via proteasome inhibition has also been shown to sensitize melanoma cells to undergo apoptosis when treated with TRAIL and other TNF family members (3, 45). Therefore, bortezomib has favorable characteristics as a potential immune sensitization drug.

Bortezomib is licensed for the treatment of multiple myeloma and is currently in trials for melanoma, ovarian, glioma, lung, lymphomas, renal cell, breast, sarcoma, colorectal, and neuroendocrine cancers (2). Preliminary data from a multicenter trial in patients with melanoma suggests that bortezomib lacks single agent activity for this malignancy (46). Melanoma is well recognized to be inherently resistant to multiple proapoptotic agents such as chemotherapy and irradiation. However, a small subset of patients with metastatic melanoma respond to a variety of immunotherapies, including high dose IL-2, whole tumor cell-based vaccines, DC vaccines, and adoptive transfer of Ag-restricted T cells (47). Lack of response to immunotherapy in the majority of patients

with melanoma may be due to the use of inefficient immunotherapy strategies, a lack of adequate recognition of tumor cells by activated immune effector cells, or a tumor cell insensitivity to the cellular cytotoxic apoptotic signals (40).

Several laboratories have demonstrated that DC can induce antitumor Ag-nonspecific cell-mediated cytotoxicity responses (19, 25–29). In the current study, we confirm that administration of Ag-unloaded DC to mice results in tumor responses, in our case, when target cells have been cosensitized using systemic treatment with bortezomib. It is not surprising that this is an Ag-independent phenomenon in this model, because bortezomib would be expected to inhibit endogenous peptide processing by the proteasome, and thereby result in decreased surface expression of tumor Ag peptides in MHC molecules. Strategies that could enhance the participation of innate effectors in antitumor responses have the obvious advantage of marshalling a large pool of rapidly inducible, Ag-nonspecific cells. Our *in vitro* correlative studies suggest an increased sensitivity of bortezomib-treated B16 cells to the lytic activity of TNF- α receptor ligation, which may be the molecular basis for the immunosensitization phenomenon. However, the role of TNF- α was not tested *in vivo* using specific knockout mice or soluble blocking reagents, and therefore may not have a role in the combined ability of DC vaccines and bortezomib to treat established B16 tumors.

In conclusion, our studies highlight that strategies aimed at increasing the activation state of immune effectors, together with pharmacological target modulation by intracellular alteration of sensitivity to apoptotic signals, may result in increased antitumor therapeutic effects. The approach used in the current studies was aimed at testing this mechanism by activating innate effectors with DC and modulating targets with the proteasome inhibitor bortezomib. Our data demonstrate that the antitumor activity of bortezomib can be enhanced by innate immune cell activation induced by DC administration, by virtue of this small molecule targeted inhibitor to sensitize cancer cells to innate effector cell-mediated lysis.

Disclosures

The authors have no financial conflict of interest.

References

- Richardson, P. G., B. Barlogie, J. Berenson, S. Singhal, S. Jagannath, D. Irwin, S. V. Rajkumar, G. Srkalovic, M. Alsina, R. Alexanian, et al. 2003. A phase 2 study of bortezomib in relapsed, refractory myeloma. *N. Engl. J. Med.* 348: 2609–2617.
- Adams, J. 2004. The proteasome: a suitable antineoplastic target. *Nat. Rev. Cancer* 4: 349–360.
- Sayers, T. J., A. D. Brooks, C. Y. Koh, W. Ma, N. Seki, A. Raziuddin, B. R. Blazar, X. Zhang, P. J. Elliott, and W. J. Murphy. 2003. The proteasome inhibitor PS-341 sensitizes neoplastic cells to TRAIL-mediated apoptosis by reducing levels of c-FLIP. *Blood* 102: 303–310.
- Sun, K., L. A. Welniak, A. Panoskaltsis-Mortari, M. J. O'Shaughnessy, H. Liu, I. Barao, W. Riordan, R. Sitcheran, C. Wysocki, J. S. Serody, et al. 2004. Inhibition of acute graft-versus-host disease with retention of graft-versus-tumor effects by the proteasome inhibitor bortezomib. *Proc. Natl. Acad. Sci. USA* 101: 8120–8125.
- Klein, J., and A. Sato. 2000. The HLA system: second of two parts. *N. Engl. J. Med.* 343: 782–786.
- Lanier, L. L. 1998. NK cell receptors. *Annu. Rev. Immunol.* 16: 359–393.
- Moretta, A., C. Bottino, M. Vitale, D. Pende, C. Cantoni, M. C. Mingari, R. Biassoni, and L. Moretta. 2001. Activating receptors and coreceptors involved in human natural killer cell-mediated cytotoxicity. *Annu. Rev. Immunol.* 19: 197–223.
- McMahon, C. W., and D. H. Raulet. 2001. Expression and function of NK cell receptors in CD8⁺ T cells. *Curr. Opin. Immunol.* 13: 465–470.
- Diefenbach, A., E. R. Jensen, A. M. Jamieson, and D. H. Raulet. 2001. Rae1 and H60 ligands of the NKG2D receptor stimulate tumour immunity. *Nature* 413: 165–171.
- Kagi, D., F. Vignaux, B. Ledermann, K. Burki, V. Depraetere, S. Nagata, H. Hengartner, and P. Golstein. 1994. Fas and perforin pathways as major mechanisms of T cell-mediated cytotoxicity. *Science* 265: 528–530.
- Clark, W. R., C. M. Walsh, A. A. Glass, F. Hayashi, M. Matloubian, and R. Ahmed. 1995. Molecular pathways of CTL-mediated cytotoxicity. *Immunol. Rev.* 146: 33–44.
- Pan, G., K. O'Rourke, A. M. Chinnaiyan, R. Gentz, R. Ebner, J. Ni, and V. M. Dixit. 1997. The receptor for the cytotoxic ligand TRAIL. *Science* 276: 111–113.
- Ribas, A., L. H. Butterfield, B. Hu, V. B. Dissette, A. Y. Chen, A. Koh, S. N. Amarnani, J. A. Glaspy, W. H. McBride, and J. S. Economou. 2000. Generation of T-cell immunity to a murine melanoma using MART-1-engineered dendritic cells. *J. Immunother.* 23: 59–66.
- Lightcap, E. S., T. A. McCormack, C. S. Pien, V. Chau, J. Adams, and P. J. Elliott. 2000. Proteasome inhibition measurements: clinical application. *Clin. Chem.* 46: 673–683.
- Comin-Anduix, B., L. G. Boros, S. Marin, J. Boren, C. Callol-Massot, J. J. Centelles, J. L. Torres, N. Agell, S. Bassilian, and M. Cascante. 2002. Fermented wheat germ extract inhibits glycolysis/pentose cycle enzymes and induces apoptosis through poly(ADP-ribose) polymerase activation in Jurkat T-cell leukemia tumor cells. *J. Biol. Chem.* 277: 46408–46414.
- Ribas, A., L. H. Butterfield, W. H. McBride, S. M. Jilani, L. A. Bui, C. M. Vollmer, R. Lau, V. B. Dissette, B. Hu, A. Y. Chen, et al. 1997. Genetic immunization for the melanoma antigen MART-1/Melan-A using recombinant adenovirus-transduced murine dendritic cells. *Cancer Res.* 57: 2865–2869.
- Inaba, K., M. Inaba, N. Romani, H. Aya, M. Deguchi, S. Ikehara, S. Muramatsu, and R. M. Steinman. 1992. Generation of large numbers of dendritic cells from mouse bone marrow cultures supplemented with granulocyte/macrophage colony-stimulating factor. *J. Exp. Med.* 176: 1693–1702.
- Ribas, A., L. H. Butterfield, W. H. McBride, V. B. Dissette, A. Koh, C. M. Vollmer, B. Hu, A. Y. Chen, J. A. Glaspy, and J. S. Economou. 1999. Characterization of antitumor immunization to a defined melanoma antigen using genetically engineered murine dendritic cells. *Cancer Gene Ther.* 6: 523–536.
- Ribas, A., J. A. Wargo, B. Comin-Anduix, S. Sanetti, L. Y. Schumacher, C. McLean, V. B. Dissette, J. A. Glaspy, W. H. McBride, L. H. Butterfield, and J. S. Economou. 2004. Enhanced tumor responses to dendritic cells in the absence of CD8-positive cells. *J. Immunol.* 172: 4762–4769.
- Ribas, A., L. H. Butterfield, B. Hu, V. B. Dissette, W. S. Meng, A. Koh, K. J. Andrews, M. Lee, S. N. Amar, J. A. Glaspy, et al. 2000. Immune deviation and Fas-mediated deletion limit antitumor activity after multiple dendritic cell vaccinations in mice. *Cancer Res.* 60: 2218–2224.
- Ribas, A., L. H. Butterfield, S. N. Amarnani, V. B. Dissette, D. Kim, W. S. Meng, G. A. Miranda, H. J. Wang, W. H. McBride, J. A. Glaspy, and J. S. Economou. 2001. CD40 cross-linking bypasses the absolute requirement for CD4 T cells during immunization with melanoma antigen gene-modified dendritic cells. *Cancer Res.* 61: 8787–8793.
- Garban, H. J., and B. Bonavida. 2001. Nitric oxide disrupts H₂O₂-dependent activation of nuclear factor κ B: role in sensitization of human tumor cells to tumor necrosis factor- α -induced cytotoxicity. *J. Biol. Chem.* 276: 8918–8923.
- Ribas, A., S. N. Amarnani, G. M. Buga, L. H. Butterfield, V. B. Dissette, W. H. McBride, J. A. Glaspy, L. J. Ignarro, and J. S. Economou. 2002. Immunosuppressive effects of interleukin-12 coexpression in melanoma antigen gene-modified dendritic cell vaccines. *Cancer Gene Ther.* 9: 875–883.
- Wargo, J. A., L. Y. Schumacher, B. Comin-Anduix, V. B. Dissette, J. A. Glaspy, W. H. McBride, L. H. Butterfield, J. S. Economou, and A. Ribas. 2005. Natural killer cells play a critical role in the immune response following immunization with melanoma-antigen-engineered dendritic cells. *Cancer Gene Ther.* 12: 516–527.
- Fernandez, N. C., A. Lozier, C. Flament, P. Ricciardi-Castagnoli, D. Bellet, M. Suter, M. Perricaudet, T. Tursz, E. Maraskovsky, and L. Zitvogel. 1999. Dendritic cells directly trigger NK cell functions: cross-talk relevant in innate anti-tumor immune responses *in vivo*. *Nat. Med.* 5: 405–411.
- van den Broeke, L. T., E. Daschbach, E. K. Thomas, G. Andringa, and J. A. Berzofsky. 2003. Dendritic cell-induced activation of adaptive and innate antitumor immunity. *J. Immunol.* 171: 5842–5852.
- Ribas, A., D. D. Vo, D. L. Weeks, B. Comin-Anduix, L. Y. Schumacher, H. J. Garban, C. McLean, J. Yang, V. B. Dissette, P. Peraza, et al. 2005. Broad antitumor protection by dendritic cells administered to CD8 α knock out mice. *Cancer Immunol. Immunother.* 13: 1–9.
- Dworacki, G., V. R. Cicinnati, S. Beckebaum, E. Pizzoferrato, T. K. Hoffmann, and A. B. De Leo. 2005. Unpulsed dendritic cells induce broadly applicable anti-tumor immunity in mice. *Cancer Biol. Ther.* 4: 50–56.
- Adam, C., S. King, T. Allgeier, H. Braumuller, C. Luking, J. Mysliwicz, A. Kriegeskorte, D. H. Busch, M. Rocken, and R. Mocikat. 2005. DC-NK cell cross talk as a novel CD4⁺ T-cell-independent pathway for antitumor CTL induction. *Blood* 106: 338–344.
- Yasuda, M., J. W. Han, C. A. Dionne, J. M. Boyd, and G. Chinnadurai. 1999. BNIP3 α : a human homolog of mitochondrial proapoptotic protein BNIP3. *Cancer Res.* 59: 533–537.
- Yook, Y.-H., K.-H. Kang, O. Maeng, T.-R. Kim, J.-O. Lee, K.-I. Kang, Y. S. Kim, S.-G. Paik, and H. Lee. 2004. Nitric oxide induces BNIP3 expression that causes cell death in macrophages. *Biochem. Biophys. Res. Commun.* 321: 298–305.
- Adonai, N., K. N. Nguyen, J. Walsh, M. Iyer, T. Toyokuni, M. E. Phelps, T. McCarthy, D. W. McCarthy, and S. S. Gambhir. 2002. Ex vivo cell labeling with ⁶⁴Cu-pyruvaldehyde-bis(N4-methylthiosemicarbazone) for imaging cell trafficking in mice with positron-emission tomography. *Proc. Natl. Acad. Sci. USA* 99: 3030–3035.
- Rosenfeld, M. G., and C. K. Glass. 2001. Coregulator codes of transcriptional regulation by nuclear receptors. *J. Biol. Chem.* 276: 36865–36868.

34. Liao, Y. P., C. C. Wang, L. H. Butterfield, J. S. Economou, A. Ribas, W. S. Meng, K. S. Iwamoto, and W. H. McBride. 2004. Ionizing radiation affects human MART-1 melanoma antigen processing and presentation by dendritic cells. *J. Immunol.* 173: 2462–2469.
35. Dodson, G. E., Y. Shi, and R. S. Tibbetts. 2004. DNA replication defects, spontaneous DNA damage, and ATM-dependent checkpoint activation in replication protein A-deficient cells. *J. Biol. Chem.* 279: 34010–34014.
36. Sax, J. K., and W. S. El-Deiry. 2003. Identification and characterization of the cytoplasmic protein TRAF4 as a p53-regulated proapoptotic gene. *J. Biol. Chem.* 278: 36435–36444.
37. Amara, R. R., F. Villinger, J. D. Altman, S. L. Lydy, S. P. O’Neil, S. I. Staprans, D. C. Montefiori, Y. Xu, J. G. Herndon, L. S. Wyatt, et al. 2001. Control of a mucosal challenge and prevention of AIDS by a multiprotein DNA/MVA vaccine. *Science* 292: 69–74.
38. Nishida, S., S. Yoshioka, S. Kinoshita-Kimoto, M. Kotani, M. Tsubaki, Y. Fujii, T. T. Tomura, and K. Irimajiri. 2003. Pretreatment with PKC inhibitor triggers TNF- α induced apoptosis in TNF- α -resistant B16 melanoma BL6 cells. *Life Sci.* 74: 781–792.
39. Marincola, F. M., E. M. Jaffee, D. J. Hicklin, and S. Ferrone. 2000. Escape of human solid tumors from T-cell recognition: molecular mechanisms and functional significance. *Adv. Immunol.* 74: 181–273.
40. Ng, C. P., and B. Bonavida. 2002. A new challenge for successful immunotherapy by tumors that are resistant to apoptosis: two complementary signals to overcome cross-resistance. *Adv. Cancer Res.* 85: 145–174.
41. Frost, P., C. P. Ng, A. Beldegrun, and B. Bonavida. 1997. Immunosenitization of prostate carcinoma cell lines for lymphocytes (CTL, TIL, LAK)-mediated apoptosis via the Fas-Fas-ligand pathway of cytotoxicity. *Cell. Immunol.* 180: 70–83.
42. Kisselev, A. F., and A. L. Goldberg. 2001. Proteasome inhibitors: from research tools to drug candidates. *Chem. Biol.* 8: 739–758.
43. Kumatori, A., K. Tanaka, N. Inamura, S. Sone, T. Ogura, T. Matsumoto, T. Tachikawa, S. Shin, and A. Ichihara. 1990. Abnormally high expression of proteasomes in human leukemic cells. *Proc. Natl. Acad. Sci. USA* 87: 7071–7075.
44. Sunwoo, J. B., Z. Chen, G. Dong, N. Yeh, C. Crowl Bancroft, E. Sausville, J. Adams, P. Elliott, and C. Van Waes. 2001. Novel proteasome inhibitor PS-341 inhibits activation of nuclear factor- κ B, cell survival, tumor growth, and angiogenesis in squamous cell carcinoma. *Clin. Cancer Res.* 7: 1419–1428.
45. Franco, A. V., X. D. Zhang, E. Van Berkel, J. E. Sanders, X. Y. Zhang, W. D. Thomas, T. Nguyen, and P. Hersey. 2001. The role of NF- κ B in TNF-related apoptosis-inducing ligand (TRAIL)-induced apoptosis of melanoma cells. *J. Immunol.* 166: 5337–5345.
46. Markovic, S. N., S. M. Geyer, F. Dawkins, W. Sharfman, M. Albertini, W. Maples, P. M. Fracasso, T. Fitch, P. Lo Russo, A. A. Adjel, and C. Erlichman. 2005. A phase II study of bortezomib in the treatment of metastatic malignant melanoma. *Cancer* 103: 2584–2589.
47. Ribas, A., L. H. Butterfield, J. A. Glaspy, and J. S. Economou. 2003. Current developments in cancer vaccines and cellular immunotherapy. *J. Clin. Oncol.* 21: 2415–2432.